Applied Catalysis B: Environmental 84 (2008) 570–576

Contents lists available at ScienceDirect

Applied Catalysis B: Environmental

journal homepage: www.elsevier.com/locate/apcatb

Novel method for preparation of high visible active N-doped TiO_2 photocatalyst with its grinding in solvent

In-Cheol Kang *, Qiwu Zhang, Shu Yin, Tsugio Sato, Fumio Saito

Institute of Multidisciplinary Research for Advanced Materials, Tohoku University, Sendai 980-8577, Japan

ARTICLE INFO

Article history:
Received 11 January 2008
Received in revised form 13 May 2008
Accepted 16 May 2008
Available online 28 May 2008

Keywords:
Surface modification
Ethanol
Current-doubling effect
TiO_2 photocatalyst
Grinding

ABSTRACT

This work is focused on improvement on the photo-catalytic activity of a N-doped TiO_2 (reference sample) by its grinding in solvent. Grinding the reference sample in solvent was performed by using a planetary mill at 200 rpm and 15 min grinding time with one of various solvents such as ethanol, ethyl acetate dehydrated (EAD), hexane and water. The ground samples were dried at 80 °C to remove the residual solvents. The prepared sample was characterized by a series of analytical methods including X-ray diffraction (XRD), specific surface area (SSA), particle size, Fourier transform infrared spectroscopy (FT-IR), thermogravimeter mass spectrometer (TG-MS), X-ray photoelectron spectroscopy (XPS), Chemiluminescence as well as the photo-catalytic activity with NO gas decomposition. The prepared sample ground in ethanol showed much improved photocatalytic activity in the wavelength of visible light region, in comparison with the activity of the reference sample. This may be due to the existence of abundant electrons on Ti^{3+}/oxygen vacancy sites, which may be generated via current-doubling effect during the dry operation. On the contrary, the sample prepared in EAD showed the worsened photocatalytic activity in visible wavelength region, due to the existence of acetate complex on the surface of the sample as a surface impurity.

1. Introduction

Intensive investigations on photo-catalyst, TiO_2, have been conducted because of its excellent functions such as water splitting, conversion of solar energy to chemical and to electrical energy, water and air purification [1–3]. However, pure TiO_2 has limited its photo-reactivity in range of ultra-violet wavelength, which is only about 3–4% in solar irradiation, due to its wide band gap energy. Therefore, much effort has been exhausted to study doping TiO_2 with non-metal [4–10] or transitional metal [11] for band gap narrowing, resulting in realization of efficient utilization of solar energy. However, there still exists the need for improving the performance of the doped sample. In addition, expensive chemicals as a starting materials and complicated process have been one of the problems in the realization of utilization of visible-active photo-catalyst.

In order to dope non-metal elements, particularly, a novel mechanochemical process has been developed and found to be effective for the achievement of high activity in visible region [5–7]. Clearly the products prepared by mechanochemical process show better photocatalytic activity than the undoped pure materials under visible irradiation region. Furthermore, it is interesting to note the photocatalytic activity of the doped sample varies depending on the preparing methods. In other words, not only the doping degree, but also other operation factors may affect the photocatalytic activity. As one example, the photocatalytic activity has been improved when the surface of photocatalyst was modified by using various solvents or organics [12–16].

The main purpose of this paper is to provide information on the improvement of photocatalytic activity of a N-doped TiO_2 by its grinding in solvent. When the doped (reference) sample was ground in solvents such as ethanol, ethyl acetate dehydrated (EAD), hexane and water, interesting results from the photo-catalytic activity and surface characterization of the samples have been observed. The product ground in ethanol shows much improved photocatalytic activity compared with the reference sample. On the contrary, the treatment with ethyl acetate dehydrated (EAD) results in reduction in photocatalytic activity. Discussion based on mainly the existence of rich electrons trapped on Ti^{3+}/oxygen vacancy sites with ethanol treatment and the effect of surface impurity from EAD treatment are conducted.

* Corresponding author. Tel.: +81 22 217 5136; fax: +81 22 217 5136.
E-mail address: kic22@andy.tagen.tohoku.ac.jp (I.-C. Kang).

0926-3373/$ – see front matter © 2008 Elsevier B.V. All rights reserved.
doi:10.1016/j.apcatb.2008.05.017

2. Experimental

2.1. Preparation of a N-doped TiO_2 (reference product)

A N-doped TiO_2 (reference product) was prepared under previous reports [5,6] simply as follows; Anatase–TiO_2 powder (anatase–TiO_2, purity-min 98.5%, Wako Pure Chem. Inc., Japan) was a starting material for grinding. A planetary ball mill (Pulverisette-7, Fritsch, Germany) was used for the grinding, and the mill consists of two set of pot made of partial stabilized zirconia (PSZ) having 45 cm^3 in inner volume, in which seven zirconia balls of 15 mm in diameter and starting materials (3.6 g) and $(NH_4)_2CO_3$ reagent (0.4 g) were put, and then the grinding was run at 700 rpm for 2 h, followed by heating operation treated at 200 °C for 1 h with increasing rate of 200 °C/h in air. Hereafter, this product is named as 'reference sample'.

2.2. Grinding the reference sample (N-doped TiO_2) in solvent

The reference sample, the N-doped TiO_2, was ground in one of the solvents; ethanol (C_2H_5OH(95); 95%, Wako Pure Chem. Indus., Lot-KLL 5241), ethyl acetate dehydrated (hereafter; EAD) ($CH_3COOC_2H_2$; 99.5%, Wako Pure Chem. Indus., Lot-DWE9906), hexane ($CH_3(CH_2)_4CH_3$; 99.5%, Wako Pure Chem. Indus., Lot; KLL-DPP9098), distilled water (hereafter water). The grinding operation was performed at relatively mild conditions as follows; the reference sample (2 g), solvent (30 ml) and balls (Φ = 5 mm; 40 g) were put into the mill pot, subsequently the grinding was started to run at 200 rpm for 15 min. After grinding operation the residual solvent was removed by heating at around 80 °C with magnetic stirring and then the sample was kept in an oven at 80 °C for 12 h.

2.3. Characterization of products

All characterizations with respect to samples were performed after drying procedure.

The phase molar ratio of anatase and rutile affects strongly on photocatalytic activity of TiO_2 [17–20]. Therefore, the phase constitute of products was determined by using X-ray diffraction analysis (XRD) (RAD-B, Rigaku Co. Ltd., Japan) using Cu Kα radiation. The phase molar ration of anatase and rutile was calculated by using peak intensity according to the Spurr and Myers method [21]:

$$W_r = \frac{1}{[1 + 0.8(I_a/I_r)]} \quad (1)$$

$$W_a = 1 - W_r \quad (2)$$

where W_a and W_r are respectively assigned to the mole ratio of anatase and rutile, I_a and I_r are assigned to the peak intensity of anatase d(1 0 1) and rutile d(1 1 0).The particle size (D) was calculated by following Scherrer's formula [22]:

$$D = \frac{0.9\lambda}{\beta_{1/2}\cos\theta} \quad (3)$$

where λ is the wavelength (0.15418 nm) of the X-ray, $\beta_{1/2}$ is line-width at medium height of anatase d(1 0 1) and rutile d(1 1 0), and θ is the diffracting angle.

The average particle size was calculated by the following equation:

$$D_{ave.} = \left(D_a \times \frac{I_a}{I_a + I_r}\right) + \left(D_r \times \frac{I_r}{I_a + I_r}\right) \quad (4)$$

where $D_{ave.}$ is the average particle size, D_a and D_r are particle sizes of anatase d(1 0 1) and rutile d(1 1 0), respectively. I_a and I_r are peak intensity of anatase d(1 0 1) and rutile d(1 1 0), respectively.

The specific surface area (SSA) of products was measured by nitrogen adsorption–desorption isothermal measurements at 77 K (ASAP-2010, Micromeritics, USA) based on a BET method.

Fourier transform infrared spectroscopy was recorded with 4 cm^{-1} resolution by an FT-IR spectrometer (FTS 7000, Mid & ATR) ranged from 500 to 4000 cm^{-1} in wavelength.

Thermogravimeter mass spectrometer (TG-MS) (Thermo Plus TG 8120, Rigaku Co. Ltd., Japan) was operated in helium atmosphere of 300 ml/min flowing rate with increasing rate of 20 °C/min to 800 °C for understanding the evaporating behavior of the products.

X-ray photoelectron spectroscopy (XPS) (PHI 5600 ESCA system, Ulvac-Phi Inc., Japan) was conducted to have the information on chemical binding energy of the products. Before and after the Ar^+ sputtering with 3 kV Ar^+ ion for 5 min on 4 mm × 4 mm area, the XPS scanning was recorded with Mg Kα X-ray by 20 times × 3cycles.

The low-level luminous intensity of chemiluminescence of singlet oxygen ($^1O_2$) was measured by a multiluminescence-spectrometer (MLA-GOLDS; Tohoku Electric Ind., Japan) at 25 °C in air. The sample was placed in the stainless steel chamber (20 mm in diameter and 10 mm in depth). The sample was irradiated for 5 s by four different types of LED light, *i.e.* UV light (375 nm in wavelength), Blue light (470 nm in wavelength), Green light (530 nm in wavelength) and Red light (630 nm in wavelength). The luminous intensity of chemiluminescence of singlet oxygen ($^1O_2$) having 634 nm in wavelength was calculated as follows: the luminous intensity of singlet oxygen was measured by using two kinds of filters λ < 620 nm and <640 nm in wavelength, respectively, and then the luminous intensity of λ < 640 nm subtracts from the luminous intensity of λ < 620 nm in wavelength.

NO gas decomposition activity of the prepared and reference samples was measured in order to examine their photocatalytic activities. The measurement was conducted as follows: the product was put on a hollow place of 20 mm × 15 mm × 0.5 mm mm on a glass holder plate and set in the center of the reactor box. A 450-W high-pressure mercury lamp (the irradiation intensity was set in 1000 μmol/(s m^2 uA)) was used as the light source, in which the wavelength was controlled by various filters, *i.e.*, Pyrex glass for cutting off the light of wavelength <290 nm, Kenko L41 Super Pro (W) filter <400 nm and Fuji, triacetyl cellulose filter <510 nm [23]. 1 ppm NO–50 vol.% air mixed gas was flowed into the reactor at flowing rate of 200 cm^3/min, and the concentration of NO gas was measured at the outlet of the reactor box (373 cm^3).

3. Results and discussion

3.1. Characterization of the products

Fig. 1 demonstrates phase constitution of products ground in each solvent at 200 rpm for 15 min. (a) is profile of reference sample, and from (b) to (e) are respectively that of product ground in ethanol, EAD, hexane and water. The marks A, R, S and Z indicate anatase, rutile, srilankite and zirconia from wear of pot and ball during grinding operation. All products show almost similar profile pattern and peak intensity. XRD results show the grinding operation and use of solvent does not change phase constitution and crystallinity.

In addition, the phase molar ratio of anatase and rutile plays an important role in photocatalytic activity due to an inducing effective separation of excited electron and hole; the P-25 is a representative product, which consists of anatase/rutile (70/30).

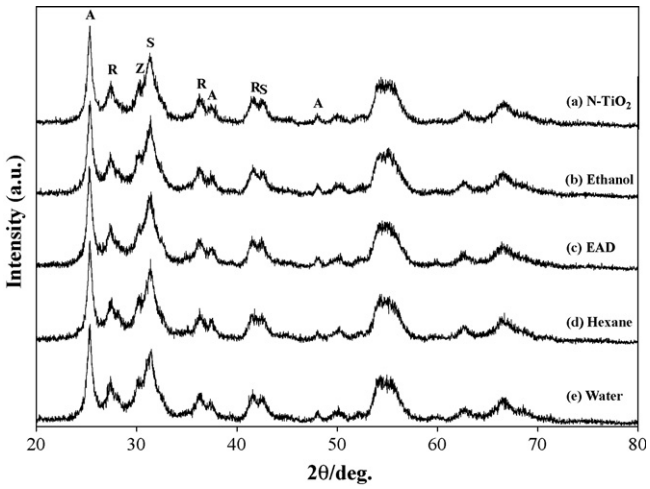

Fig. 1. XRD profiles of products depending on the solvent used: (a) reference sample, (b–e) are that of the product ground in (b) ethanol, (c) ethyl acetate dehydrated (EAD), (d) hexane and (e) water (A: anatase, R: rutile, S: srilankite, Z: zirconia).

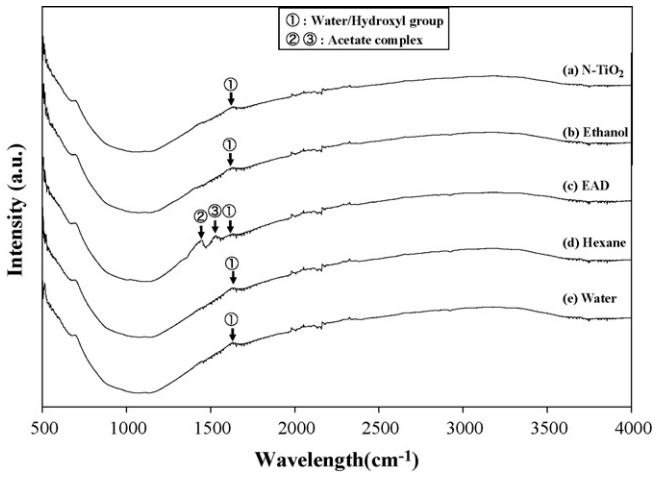

Fig. 2. FT-IR profiles of the products: (1) indicates water/hydroxyl group, (2) and (3) indicate acetate complex.

Table 1
Phase molar ratio and specific surface area and average particle size of product with solvent used

The used solvent	Phase ratio (mol%)		Specific surface area ($m^2\ g^{-1}$)	Average particle size (nm)
	Anatase	Rutile		
(a) None (reference)	0.63	0.37	55.41	12.16
(b) Ethanol	0.62	0.38	61.68	11.79
(c) Ethyl acetate dehydrated (EAD)	0.64	0.36	56.77	11.84
(d) Hexane	0.65	0.35	60.46	11.04
(e) Water	0.62	0.38	62.08	11.65

Furthermore, the particle size and specific surface area are also an important factor in photocatalytic activity because the smaller particle size and the higher SSA value induce better absorbability of hydroxyl/water on surface of product, which plays as an active oxidizer in photocatalytic reaction [24]. In Table 1, it is noted that the phase molar ratio of anatase/rutile with the solvent used, resulting in no significant difference in phase molar ratio of anatase/rutile with (0.62–0.65)/(0.38–0.35). And the average particle size and specific surface area of all products are also almost similar as 11–12 nm in diameter and 55.41–62.08 $m^2\ g^{-1}$. From these results, it can be concluded that the grinding operation (with 200 rpm for 15 min) and use of solvent did not give evident effect on the change of phase structure, particle size and specific surface area.

Fig. 2 shows the FT-IR patterns of the samples treated with solvents. Except the sample (c) ground in EAD, the others represent similar spectra, where mark (1) located at around 1630 cm^{-1} is assigned to water molecule/hydroxyl groups [25,26], without any other clear bonding peaks. In the spectrum of the sample ground in EAD, two peaks of marks (2) and (3) located at 1440 and 1540 cm^{-1} are assigned to acetate complex (COO^-) [25,26]. As for the hydroxyl group, compared with other samples, the peak intensity of the sample (c) is much lower, that is attributed to the replacement of surface water/hydroxyl groups by acetate complex during grinding operation, resulting in reduction of water/hydroxyl group concentration and generation of surface impurities. This result is well demonstrated also in TG-MS result (Fig. 3).

Fig. 3 shows evaporating behavior of product recorded by TG-MS in helium flowing. Both the samples (a) and (b), which are the reference sample and the sample ground in ethanol, represent similar evaporating behavior of H_2O composition. On the other hand, the sample (c) ground in EAD shows evidently different evaporating pattern from that of the two (a and b). Decrease in the peak intensity of H_2O composition and appearance of CO_2 composition around from 300 °C are observed and this may be attributed to the decomposition of acetate complex adsorbed on TiO_2 surface, as shown in Fig. 2. Furthermore, compared with the reference sample, its lower amount of H_2O evaporation is attributed to the replacement of surface water/hydroxyl groups by acetate complex during grinding in EAD. These TG-MS results are well consistent with that of FT-IR analysis shown in Fig. 2.

Fig. 4 displays chemical binding energy of N1s and C1s with solvents used and before/after Ar^+ sputtering operation. The profiles (A) and (C) are those obtained before Ar^+ sputtering operation, while the profiles (B) and (D) are those obtained after Ar^+ sputtering. In the patterns (A) and (B), the peaks located at 396 and 400.1 eV are assigned to Ti–N and N–O/N–N binding energy, respectively. There is not any change in binding energy and/or peak intensity observed on the samples, irrespective of the solvent and grinding operation. In other words, treatment with varied solvents and soft grinding operation does not alter the N-doped state. With respect to carbon binding energy, noticeable surface modifications by grinding in solvent are observed. In the patterns (C) and (D), the C–C bonding located at 285 eV is assigned to adventitious elemental carbon [27,28], and C–O bonding located at 288.6 eV is assigned to carbonate species [28,29], of which the generation was caused through the replacement of Ti site by C from $(NH_4)_2CO_3$ reagent during preparing the reference sample. Compared with other samples, a strong peak with C–O bonding at 288.6 eV has been observed in the (c) sample. This is ascribed to the absorbed acetate complex on TiO_2 surface during grinding in EAD, of which the existence was well identified in Figs. 2 and 3. It is interesting to note, after sputtering, that such strong peak becomes weak to the same state as other samples. This means that the acetate complex composition exists on the surfaces only.

3.2. Optical property of the products

It is recognized that the singlet oxygen($^1O_2$), which can be generated by the band gap excitation of semiconductors in air, plays an important role in photocatalytic reaction. In general, singlet oxygen shows a dimole emission (5) and a monomole

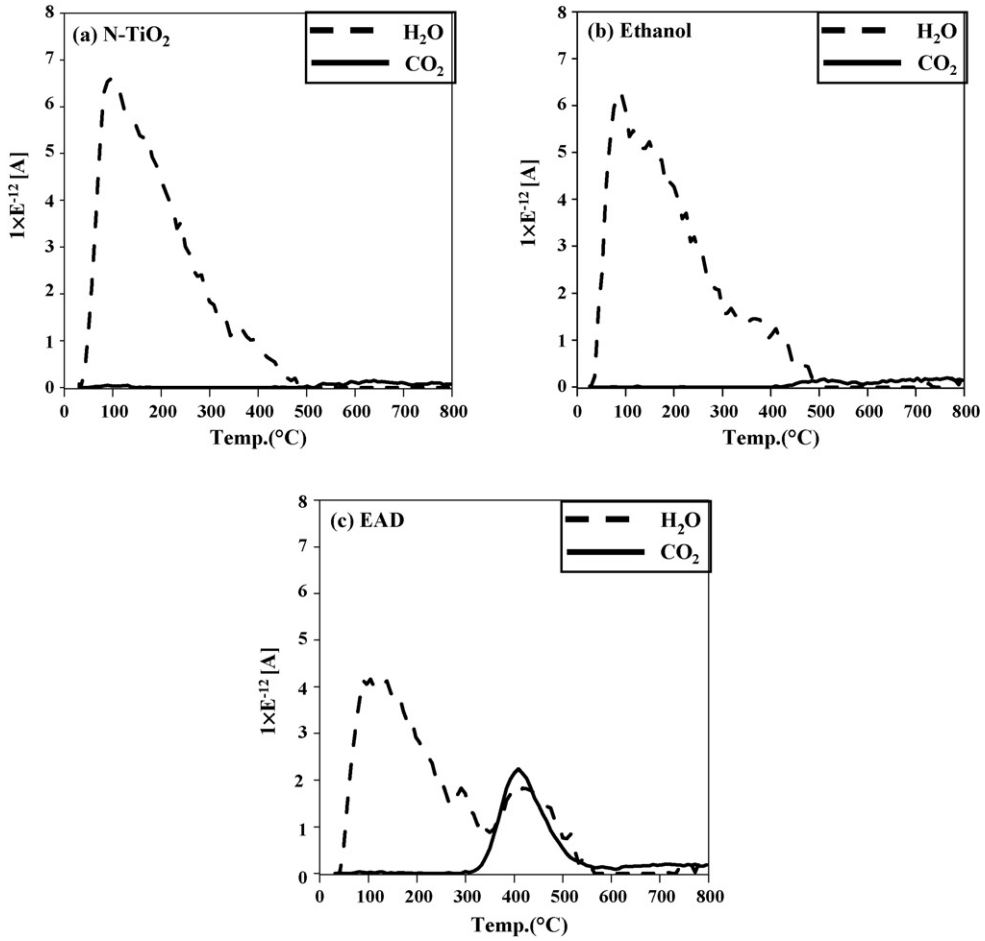

Fig. 3. TG-MS profiles of products: (a) reference sample (N-TiO_2), (b) sample ground in ethanol and (c) in EAD.

emission (6); [30]:

$$^1O_2 + {}^1O_2 \rightarrow 2^3O_2 + h\nu \qquad (634 \text{ and } 703 \text{ nm}) \tag{5}$$

$$^1O_2 \rightarrow {}^3O_2 + h\nu \qquad (1270 \text{ nm}) \tag{6}$$

And its weak chemiluminescence in the range of visible irradiation (634 nm) was recorded by using the filter to cut off the emission attributed to the carbonyl compounds [31].

Fig. 5 represents the luminous intensity of singlet oxygen of products against different irradiation wavelength: 375 nm (UV light), 470 nm (Blue light), 530 nm (Green light) and 630 nm (Red light). Compared with reference sample (a), clear increase in the luminous intensity of product (b) ground in ethanol has been observed with irradiations by all the used lights. Especially, evident emission of singlet oxygen by green light irradiation, which is almost unobservable from the reference sample, is obtained by ethanol treatment. In other words, it means that more electrons can be obtained even by green visible irradiation from the product (b). On the other hand, the product (c) ground in EAD shows weak luminous intensity compared with reference product (a) with all irradiation and emits singlet oxygen just to UV irradiation.

Although not shown here, all products shows similar UV–vis curves, indicating that the band gap structure maintains the same state, without formation of sub-band structure in product (b) ground in ethanol. Subsequently, it means that the difference in luminous intensity of singlet oxygen is not related to the change of phase constitution, specific surface area, particle size and band structure. As for this phenomenon, interpretation is performed on the basis of previous literatures. First, the phenomenon which electrons can be excited to conduction band by relatively weak irradiation energy (from Fig. 5) implies that electrons stay near to bottom of conduction band. Indeed, then, how does these electrons stay at that position? According to suggestion of Bilmes et al. [32] and Sakai et al. [33], oxygen vacancies offer sub-band level in the band gap. And Henglein and Bunsenges [34] and Ohno et al. [35] proposed that Ti^{3+} and oxygen vacancies sites located at 0.75–1.18 eV below from bottom of conduction band. Moreover, Komaguchi et al. [36], Cronemeyer [37] and Breckenridge and Hosler [38] reported the electrons trapped on Ti^{3+} and oxygen vacancies sites can be excited to conduction band even by relatively weak irradiation energy in comparison with that of band gap energy.

According to current-doubling effect [39–41], during grinding operation of N-TiO_2 in ethanol, the ethanol reacts with hydroxyl group (–OH) adsorbed on surface, resulting in generation of ethoxide ($C_2H_5O^-$). And during drying operation on hot-plating the sample was irradiated by indoor light, so that it may cause photo-generated holes and electrons. The holes are trapped by ethoxide, and the hole-trap species ($C_2H_5O^\bullet$) with an electron energy level above the bottom of the conduction band is formed. Thus, the hole-trap species can inject an electron into the conduction band [40]. Accordingly, interaction on the surfaces between OH^-(a) + C_2H_5OH(l) occurs in the grinding operation. Then, the reaction product ethoxide captures the photo-generated holes in valence band to form $C_2H_5O^\bullet$(a). The hole-capture species ($C_2H_5O^\bullet$) is decomposed to inject electrons to conduction band of catalyst.

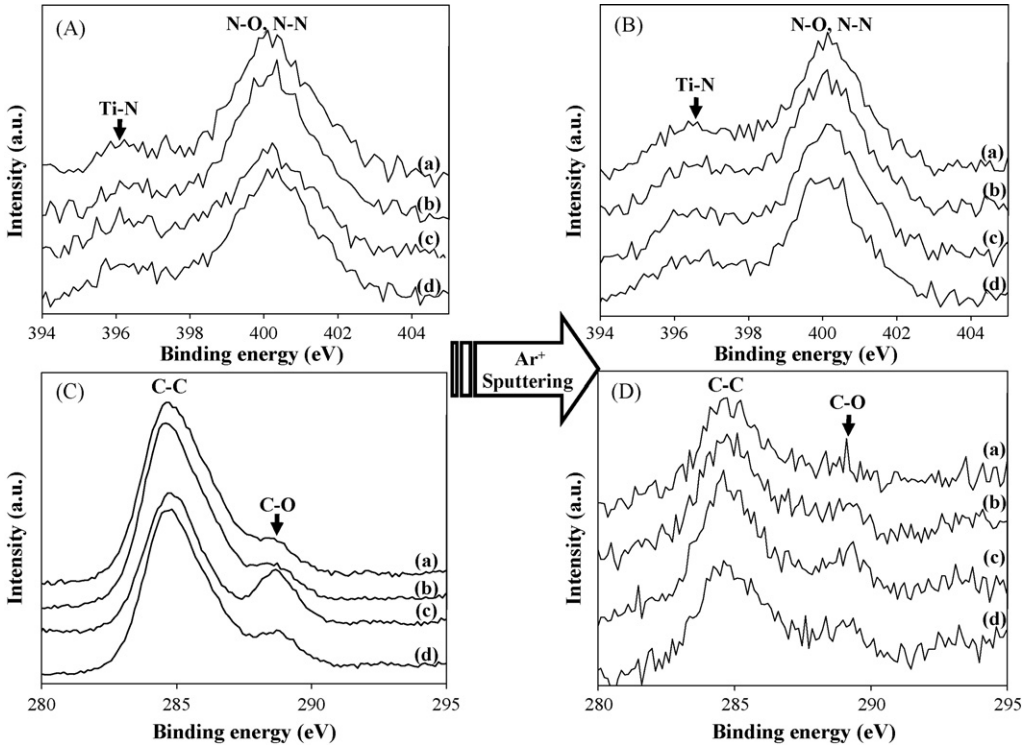

Fig. 4. XPS profiles of products: ((A) and (B): N1s binding energy, (C) and (D): C1s binding energy; (A) and (C): before sputtering operation, (B) and (D): after sputtering operation), (a–d) are respectively that of reference product and products ground in ethanol, EAD and hexane.

Of course, some of the electrons in conduction band might be recombined with hole as usually. However, the amount of electron is more than that of the hole due to the decomposition. Therefore, the uncombined electrons should be trapped on somewhere. Ti^{3+} and oxygen vacancy sites localized at 0.75–1.18 eV below from bottom of conduction band [34,35] is the possible positions. The electrons trapped on Ti^{3+} and oxygen vacancy sites could be excited to conduction band even by weaker irradiation energy than that of the band gap energy [36–38]. Therefore, this product could generate abundant electrons even against green visible light after the treatment with ethanol. This might be the reason why the sample prepared in ethanol shows stronger luminous intensity of singlet oxygen against green light as well as UV light, compared to that of the reference product.

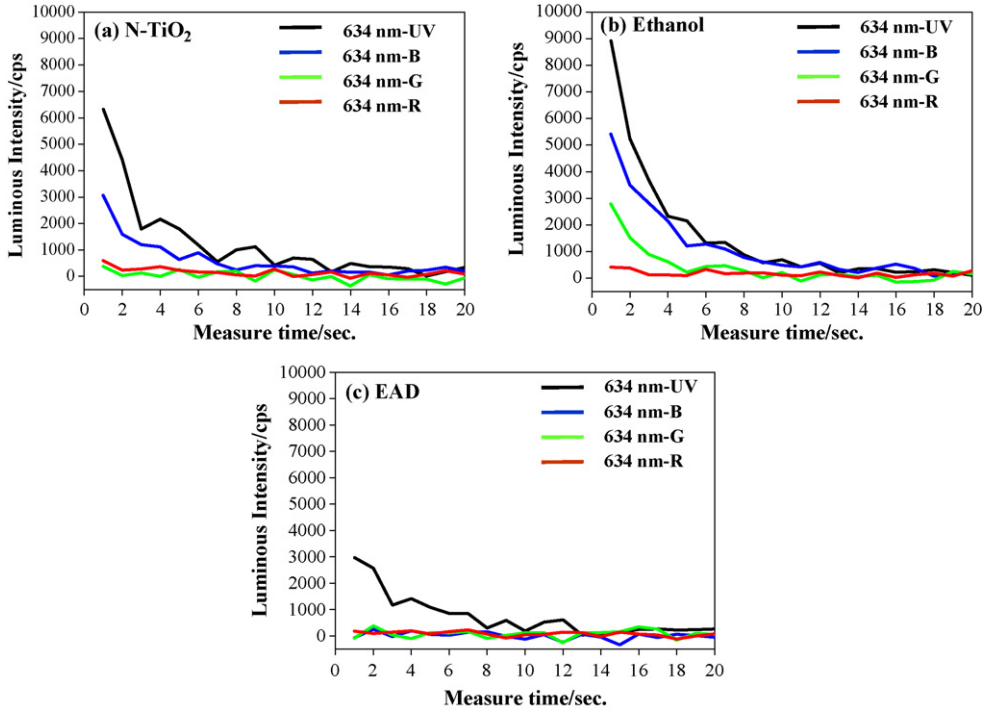

Fig. 5. The luminous intensity of chemiluminescence of singlet oxygen depending on the wavelength of light irradiation.

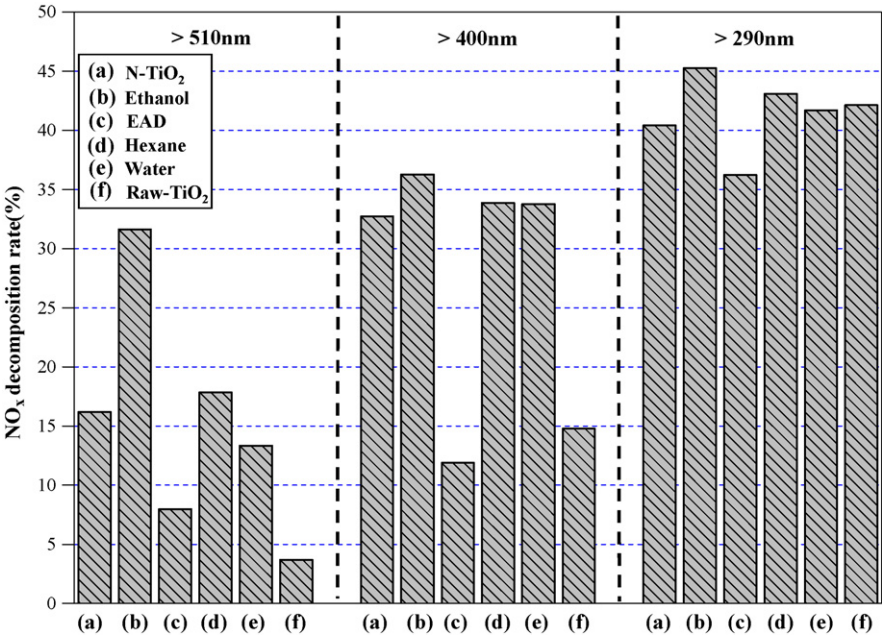

Fig. 6. NO gas decomposition activity of products: (a) reference sample (N-TiO_2), (b) sample ground in ethanol, (c) in EAD, (d) in hexane, (e) in water and (f) pure anatase TiO_2.

On the contrary, the reason with respect to the weakness of luminous intensity of product (c) ground in EAD is due to the existence of surface impurity via replacement of water/hydroxyl group by acetate complex.

3.3. Characterization of photocatalytic activity

Fig. 6 shows NO gas decomposition activity of the prepared and the reference samples. Samples (a–f) are denoted as reference sample, samples prepared in ethanol, EAD, hexane, water and raw-TiO_2, respectively. The activity of the reference sample (a) under visible light irradiation is much higher than that of the raw-TiO_2 (f), due to the doping effect. It is very interesting to note that the photocatalytic activities in visible wavelength of the prepared samples (b) and (e) are strongly dependent on the solvent used. The photocatalytic activity of the sample (b) ground in ethanol has drastically increased by two times more than that of the reference sample (a). On the contrary, the activity of the sample (c) is much lower than that of the sample (a). The result of photocatalytic activity of both product (b) and (c) corresponds to the results of luminous intensity of singlet oxygen. In other words, the product (b) can show higher photocatalytic activity in all of wavelength region due to existence of abundant electrons near to conduction band. On the other hand, as for the other products (d) and (e) ground in hexane and water, there is not any distinct difference in comparison with that of the reference sample (a).

4. Conclusions

Treatment of the N-doped sample with solvents is found to affect significantly its photocatalytic activity. When ethanol is used as a solvent, much improvement in the activity of the sample has been obtained. This offers an easy way to provide a visible light active sample prepared through the mechanochemical process. On the contrary, when ethyl acetate is used as a solvent, interaction on the particle surfaces induces impurity of acetate complex, leading in decrease of the activity significantly.

Acknowledgment

One of the authors (I.C.K.) is grateful to the Korean Government (MOST) for the financial support provided through the Korea Science and Engineering Foundation Grant (no. 2005-215-D00146).

References

[1] A. Fujishima, K. Honda, Nature 238 (1972) 37–38.
[2] B. Öregan, M. Grätzel, Nature 353 (1991) 737–740.
[3] A. Linsebigler, G. Lu, J.T. Yates Jr., Chem. Rev. 95 (1995) 735–758.
[4] S.U.M. Khan, M. Al-shahry, W.B. Ingler Jr., Science 297 (2002) 2243–2245.
[5] I.C. Kang, Q. Zhang, J. Kano, S. Yin, T. Sato, F. Saito, J. Photochem. Photobiol. A: Chem. 189 (2007) 232–238.
[6] S. Yin, K. Ihara, M. Komatsu, Q. Zhang, F. Saito, T. Kyotani, T. Sato, Solid State Commun. 137 (2006) 132–137.
[7] J. Wang, Q. Zhang, S. Yin, T. Sato, F. Saito, J. Phys. Chem. Solid 68 (2007) 189–192.
[8] R. Asahi, T. Morikawa, T. Ohwaki, K. Aoki, Y. Taga, Science 293 (2001) 269–271.
[9] L. Lin, W. Lin, J.L. Xie, Y.X. Zhu, B.Y. Zhao, Y.C. Xie, Appl. Catal. B: Environ. 75 (2007) 52–58.
[10] X. Hong, Z. Wang, W. Cai, F. Lu, J. Zhang, Y. Yang, N. Ma, Y. Liu, Chem. Mater. 17 (2005) 1548–1552.
[11] M. Anpo, M. Takeuchi, J. Catal. 216 (2003) 505–516.
[12] D. Jiang, Y. Xu, B. Hou, D. Wu, Y. Sun, J. Solid state Chem. 180 (2007) 1787–1791.
[13] E. Ukaji, T. Furusawa, M. Sato, N. Suzuki, Appl. Surf. Sci. 254 (2007) 563–569.
[14] J.C. Yu, J. Yu, J. Zhao, Appl. Catal. B: Environ. 36 (2002) 31–43.
[15] S.X. Li, F.Y. Zheng, W.L. Cai, A.Q. Han, Y.K. Xie, J. Hazard. Mater. B 135 (2006) 431–436.
[16] J.C. Yu, W. Ho, J. Yu, S.K. Hark, K. Iu, Langmuir 19 (2003) 3889–3896.
[17] A. Bojinova, R. Kralchevska, I. Poulios, C. Dushkin, Mater. Chem. Phys. 106 (2007) 187–192.
[18] J. Yu, J.C. Yu, M.K.P. Leung, W. Ho, B. Cheng, X. Zhao, J. Zhao, J. Catal. 217 (2003) 69–78.
[19] J. Yu, L. Zhang, B. Cheng, Y. Su, J. Phys. Chem. C 111 (2007) 10582–10589.
[20] J. Yu, Y. Su, B. Cheng, Adv. Funct. Mater. 17 (2007) 1984–1990.
[21] R.A. Spurr, W. Myers, Anal. Chem. 29 (1957) 760–762.
[22] Z. Wang, W. Cai, X. Hong, X. Zhao, F. Xu, C. Cai, Appl. Catal. B: Environ. 57 (2005) 223–231.
[23] S. Yin, H. Hasegawa, D. Maeda, M. Ishitsuka, T. Sato, J. Photochem. Photobiol. A: Chem. 163 (2004) 1–8.
[24] J. Yu, H. Yu, B. Cheng, M. Zhou, X. Zhao, J. Mol. Catal. A: Chem. 253 (2006) 112–118.
[25] W.C. Wu, C.C. Chuang, J.L. Lin, J. Phys. Chem. B 104 (2000) 8719–8724.
[26] G.A.M. Hussein, N. Sheppard, M.I. Zaki, R.B. Fahim, J. Chem. Soc., Faraday Trans. 87 (1991) 2661–2668.
[27] W. Ren, Z. Ai, F. Jia, L. Zhang, X. Fan, Z. Zou, Appl. Catal. B: Environ. 69 (2007) 138–144.

[28] Y. Li, D. Hwang, N. Lee, S. Kim, Chem. Phys. Lett. 404 (2005) 25–29.
[29] S. Sakthivel, H. Kisch, Angew. Chem. Int. Ed. 42 (2003) 4908–4911.
[30] J.R. Knofsky, Chem. Biol. Interact. 70 (1989) 1–28.
[31] T. Miyazawa, K. Fujimoto, M. Kinoshita, R. Usuki, J. Am. Oil Chem. Soc. 71 (1994) 343–344.
[32] S.A. Bilmes, P. Mandelbaum, F. Alvarez, N.M. Victoria, J. Phys. Chem. B 104 (2000) 9851–9858.
[33] Y. Sakai, S. Ehara, Jpn. J. Appl. Phys. Part 2 40 (2001) L773–L775.
[34] A. Henglein, B. Bunsenges, Phys. Chem. 86 (1982) 241–244.
[35] T. Ohno, K. Sarukawa, K. Tokieda, M. Matsumura, J. Catal. 203 (2001) 82–86.
[36] K. Komaguchi, H. Nakano, A. Araki, Y. Harima, Chem. Phys. Lett. 428 (2006) 338–342.
[37] D.C. Cronemeyer, Phys. Rev. 113 (1959) 1222–1226.
[38] R.G. Breckenridge, W.R. Hosler, Phys. Rev. 91 (1953) 793–802.
[39] A. Yamakata, T.A. Ishibashi, H. Onishi, J. Phys. Chem. B 106 (2002) 9122–9125.
[40] W.P. Gomes, T. Freund, S.R. Morrison, J. Electrochem. Soc. 115 (1968) 818–823.
[41] O.I. Micic, Y. Zhang, K.R. Cromack, A.D. Trifunac, M.C. Thurnauer, J. Phys. Chem. 97 (1993) 13284–13288.